

**IMMOBILIZED TiO<sub>2</sub>/CHITOSAN LAYERED SYSTEM INCORPORATING  
REACTIVE RED 4 DYE FOR THE PHOTOCATALYTIC DEGRADATION  
OF PHENOL**

by

**SUMIYYAH BINTI SABAR**

**Thesis submitted in fulfillment of the requirements for the degree of  
Doctor of Philosophy**

**April 2013**

## ACKNOWLEDGEMENT

First and foremost I would like to convey my sincere appreciation to my supervisor, Professor Dr. Mohd Asri Nawawi, for his guidance, advice, critics, and encouragement throughout the course of this work. I acknowledge the financial support provided by Universiti Sains Malaysia (USM) in the form of USM Fellowship scheme and Research University Postgraduate Research Grant Scheme (USM-RU-PGRS, 1001/PKIMIA/842070).

My special thanks go to Professor Dr. Wan Saime Wan Ngah and Professor Dr. Bassim H. Hameed for their useful discussion and motivation. For my laboratory works, I am indebted to all laboratory personnel particularly to Mr. Ariffin, Mrs. Norhayati, Mrs. Asma, Mr. Sunjay, Mr. Zamri, Mrs. Arlita, Mr. Johari and Miss Jamilah for their excellent and prompt services. I would also like to thank my colleagues, Dr. Ali, Wan Izhan, Ismariza, Ying Shin, Nazihah, Salmiah, Sharin, Lelifajri, Sheilatina, Karam, Fathanah, Dr. Mohammad, Fifi, Gazala and Bahiyah for their sincere assistances and useful discussions. Not forgetting all the respective lecturers and staffs of School of Chemical Sciences, School of Physics and Institute of Postgraduate Studies (IPS) for the help given, either directly or indirectly.

Last but not least, I would like to express my boundless appreciation to my beloved husband, Adlizan Abd. Rashid; father, Associate Professor Dr. Sabar Bauk; and mother, Sharifah Mohammed Noor, for their never-ending love, support, understanding, and patience throughout the duration of my study. The same goes to my lovely daughter, Nur Aisyah Adlizan, siblings and in-law family. May Allah accept all these efforts as ibadah to Him and delivers us all in His Jannah.

## TABLE OF CONTENTS

	Page
Acknowledgement	ii
Table of Contents	iii
List of Tables	xi
List of Figures	xiii
List of Symbols and Abbreviations	xx
Abstrak	xxii
Abstract	xxiv

## CHAPTER ONE – INTRODUCTION

1.1	Background	1
1.2	Photocatalysis	2
1.2.1	Definition	2
1.2.2	Principles of a heterogeneous photocatalysis	4
1.3	Titanium Dioxide (TiO <sub>2</sub> )	7
1.3.1	General	7
1.3.2	Properties of TiO <sub>2</sub> semiconductor	8
1.3.3	TiO <sub>2</sub> in photocatalysis	10
1.3.4	Drawbacks of TiO <sub>2</sub> photocatalyst	11
1.4	Modification of TiO <sub>2</sub>	12
1.4.1	Immobilization of TiO <sub>2</sub>	13
1.4.2	Combination with adsorbents	15
1.4.3	Dye-modified TiO <sub>2</sub>	15

1.5	Chitosan (CS) biopolymer	21
1.5.1	Properties of CS	21
1.5.2	Applications of CS	22
1.5.3	Works related to CS with TiO <sub>2</sub> semiconductor	23
1.6	Phenol as a model pollutant	24
1.7	Problem statements	30
1.8	Research objectives	31

## **CHAPTER TWO – MATERIALS AND METHODS**

2.1	Chemicals and reagents	34
2.2	Instruments and equipment	35
2.3	Preparation of stock solutions	36
2.3.1	Reactive Red 4 (RR4) dye	36
2.3.2	Phenol	37
2.4	Experimental set-up	37
2.4.1	Adsorption system set-up	37
2.4.2	Irradiation system set-up	39
2.4.3	Mineralization study	40
2.5	Fabrication of the layered system	40
2.5.1	Preparation of solid support	40
2.5.2	Preparation of immobilized CS	40
2.5.3	Preparation of RR4-CS plates	41
2.5.4	Preparation of immobilized TiO <sub>2</sub> layer	41
2.6	Characterizations	42
2.6.1	Scanning electron microscopy (SEM)	42

2.6.2	Surface area and porosity analysis	43
2.6.3	Fourier transform infrared (FTIR) spectroscopy	43
2.6.4	Adhesion and strength test	43
2.6.5	UV-Visible diffuse reflectance spectroscopy (DRS)	44
2.6.6	Voltammetric analysis	45
2.6.7	Photoluminescence (PL) spectroscopy analysis	45
2.6.8	Total organic carbon (TOC) analysis	45
2.7	Batch adsorption experiments of RR4 dye by the immobilized CS/glass system	46
2.7.1	Effect of adsorbent loading	47
2.7.2	Effect of pH	48
2.7.3	Effect of initial dye concentration and contact time	48
2.7.4	Equilibrium adsorption isotherms	48
2.7.5	Thermodynamic studies	49
2.8	Photocatalytic performance of the TiO <sub>2</sub> /CS layered system incorporating RR4 dye	49
2.9	Fabrication of TiO <sub>2</sub> /CS layered system incorporating RR4 dye	51
2.9.1	Optimization of TiO <sub>2</sub> loading	51
2.9.1(a)	Effect of TiO <sub>2</sub> loading on the photocatalytic degradation of phenol	51
2.9.1(b)	Oxidation of CS sub-layer	51
2.9.2	Optimization of aeration flow rate	52
2.9.3	Generation of macro-pores on the TiO <sub>2</sub> layer	52
2.9.3(a)	Diffusion of pollutant molecules	52
2.9.3(b)	Penetration of light and oxidative radicals	53

2.9.4	Photo-etching of the immobilized photocatalyst system	53
2.9.5	Photocatalytic degradation of RR4 dye by the immobilized layered TiO <sub>2</sub> /cross-linked CS derivatives system	54
2.10	Evaluation of the TiO <sub>2</sub> /CS layered system incorporating RR4 dye for the photocatalytic degradation of phenol	55
2.10.1	Control experiments	55
2.10.2	Effect of pH	56
2.10.3	Effect of initial phenol concentration	56
2.11	Mechanistic study	56
2.11.1	Effect of radical quenchers	56
2.11.2	Detection of hydroxyl radicals (OH <sup>•</sup> )	57
2.12	Photocatalyst reusability	58
2.12.1	Comparison between TiO <sub>2</sub> /glass, TiO <sub>2</sub> /CS/glass and TiO <sub>2</sub> /RR4-CS/glass systems	58
2.12.2	Effect of initial dye concentration	58
2.12.3	Re-treatment of the TiO <sub>2</sub> /RR4-CS layered system	59
2.13	Mineralization study	59
2.14	Identification and determination of phenol's intermediates	60

### **CHAPTER THREE – RESULTS AND DISCUSSION: ADSORPTION OF REACTIVE RED 4 (RR4) DYE BY IMMOBILIZED CS ON GLASS PLATES**

3.1	Introduction	61
3.2	Characterization of immobilized CS	62
3.2.1	SEM	62
3.2.2	Surface area and porosity analysis	65

3.2.3	FTIR spectra	66
3.2.4	Adhesion and strength test	68
3.3	Batch adsorption experiments of RR4 dye by the immobilized CS/glass system	69
3.3.1	Effect of adsorbent loading	69
3.3.2	Effect of pH	70
3.3.3	Effect of initial dye concentration and contact time	73
3.3.4	Adsorption kinetic studies	75
3.3.4(a)	Pseudo-first-order model	75
3.3.4(b)	Pseudo-second-order model	77
3.3.4(c)	Intraparticle diffusion model	79
3.3.5	Equilibrium adsorption isotherms	81
3.3.5(a)	Langmuir isotherm model	83
3.3.5(b)	Freundlich isotherm model	87
3.3.6	Thermodynamics	90

## **CHAPTER FOUR – RESULTS AND DISCUSSION: CHARACTERIZATION AND FABRICATION OF TiO<sub>2</sub>/CS LAYERED SYSTEM INCORPORATING RR4 DYE**

4.1	Introduction	92
4.2	Characterization of RR4 dye	93
4.2.1	UV-Vis DRS spectral analysis	93
4.2.2	Electrochemical properties	95
4.3	Characterization of the photocatalyst systems	97
4.3.1	UV-Vis DRS spectral analysis	97

4.3.2	PL spectral analysis	97
4.3.3	Leachability of dissolved organic matter via TOC analysis	99
4.3.4	SEM	104
4.4	Optimization of TiO <sub>2</sub> loading	106
4.4.1	Effect of TiO <sub>2</sub> loading on the photocatalytic degradation of phenol	106
4.4.2	Oxidation of CS sub-layer	109
4.5	Optimization of aeration flow rate	112
4.6	The role of macro-pores	114
4.6.1	Enhancing the diffusion of water pollutants	116
4.6.2	Enhancing the diffusion of oxidative radicals	118
4.7	Photo-etching of the immobilized photocatalyst system	120
4.8	Photocatalytic degradation of RR4 dye by the immobilized layered TiO <sub>2</sub> /cross-linked CS derivatives system	122

## **CHAPTER FIVE – RESULTS AND DISCUSSION: PHOTOCATALYTIC DEGRADATION OF PHENOL BY THE IMMOBILIZED TiO<sub>2</sub>/CS LAYERED SYSTEM INCORPORATING RR4 DYE**

5.1	Introduction	130
5.2	Photocatalytic performance of the TiO <sub>2</sub> /RR4-CS layered system for the removal of phenol	131
5.2.1	Control experiments	131
5.2.2	Effect of pH	134
5.2.3	Effect of initial phenol concentration	137
5.3	Mechanistic study	139



5.3.1	Effect of radical quenchers	139
5.3.2	Detection of hydroxyl radicals (OH <sup>•</sup> )	143
5.3.3	Proposed mechanisms	146
5.4	Catalyst reusability	150
5.4.1	Comparison between the immobilized photocatalyst systems (TiO <sub>2</sub> /glass, TiO <sub>2</sub> /CS/glass and TiO <sub>2</sub> /RR4-CS/glass)	150
5.4.2	Effect of initial dye concentration	153
5.4.3	Re-treatment of the TiO <sub>2</sub> /RR4-CS photocatalyst system	155
5.5	Mineralization study	156
5.6	Identification and determination of phenol's intermediates	159
5.6.1	Identification of phenol's intermediates	159
5.6.2	Proposed degradation pathways	165

## **CHAPTER SIX – CONCLUDING REMARKS AND SUGGESTIONS FOR FUTURE STUDIES**

6.1	Conclusions	168
6.1.1	Adsorption of Reactive Red 4 (RR4) dye by immobilized CS on glass plates	168
6.1.2	Characterization and fabrication of TiO <sub>2</sub> /CS layered system incorporating RR4 dye	170
6.1.3	Photocatalytic degradation of phenol by the immobilized TiO <sub>2</sub> /CS layered system incorporating RR4 dye	171
6.1.4	Final remarks	173
6.2	Suggestions for future studies	173

## **REFERENCES**

175

## **APPENDICES**

## **LIST OF PUBLICATIONS AND CONFERENCES**

## LIST OF TABLES

		Page
Table 1.1	Related work on dye-modified TiO <sub>2</sub> for the photocatalytic degradation of organic pollutants.	18
Table 1.2	Principal properties of CS in relation to its use in water and waste treatment applications (Renault <i>et al.</i> , 2009).	23
Table 1.3	Recent studies on the applications of TiO <sub>2</sub> -CS in heterogeneous photocatalysis.	25
Table 1.4	Summary of recent studies on phenol degradation by TiO <sub>2</sub> in heterogeneous photocatalysis.	29
Table 3.1	Textual characteristics of immobilized CS layer at different adsorbent loadings.	65
Table 3.2	The time taken to reach equilibrium for the RR4 adsorption by CS/glass and its amounts adsorbed at various initial dye concentrations.	74
Table 3.3	The pseudo-first-order constants and linear regression coefficients at different RR4 concentrations.	76
Table 3.4	The pseudo-second-order constants and linear regression coefficients at different RR4 concentrations.	78
Table 3.5	The intraparticle diffusion constants and linear regression coefficients at different RR4 concentrations.	81
Table 3.6	The Langmuir constants and linear regression coefficients for the adsorption of RR4 by air-dried and oven-dried CS/glass.	85
Table 3.7	Comparison of maximum adsorption capacities ( $q_{max}$ ) of various adsorbents for RR4 dye.	86
Table 3.8	The Freundlich constants and linear regression coefficients for the adsorption of RR4 by air-dried and oven-dried CS/glass.	89
Table 3.9	The thermodynamic parameters and linear regression coefficient for the adsorption of RR4 by CS/glass.	91

Table 4.1      The thickness of immobilized TiO<sub>2</sub> layer at different TiO<sub>2</sub> loadings.      104

Table 5.1      The main intermediates formed during the photocatalytic degradation of phenol by TiO<sub>2</sub>/CS layered system (Jawad and Nawi, 2011).      162

## LIST OF FIGURES

		Page
Figure 1.1	A Scopus database literature survey of research articles published on photocatalysis from 2002 to 2012 (the survey does not include patents).	3
Figure 1.2	Schematic illustration of the photoinduced hole and electron over photon activated semiconductor photocatalyst.	6
Figure 1.3	Band positions of several semiconductors in contact with aqueous electrolyte at pH 1 (Gratzel, 2001).	7
Figure 1.4	Bulk crystalline structures of the (a) rutile, (b) anatase, and (c) brookite type TiO <sub>2</sub> (Janisch <i>et al.</i> , 2005)	9
Figure 1.5	Mechanism of photoinduced hole and electron on the surface of TiO <sub>2</sub> photocatalyst.	11
Figure 1.6	Mechanism of the dye-sensitized TiO <sub>2</sub> photocatalyst.	17
Figure 1.7	Scheme of chemical deacetylation of chitin to produce chitosan.	21
Figure 2.1	Chemical structure of Reactive Red 4 (RR4) dye.	37
Figure 2.2	Schematic diagram of experimental set-up for the adsorption of RR4 and/or phenol (A) immobilized plate, (B) RR4 and/or phenol aqueous solution, (C) glass reactor cell, (D) Pasteur pipette, (E) PVC tubing, (F) air flow-meter, (G) aquarium pump, and (H) box.	38
Figure 2.3	Schematic diagram of experimental set-up for the irradiated condition. (A) 45 W compact fluorescent lamp, (B) glass reactor cell, (C) immobilized plate, (D) RR4 and/or phenol aqueous solution, (E) aeration supplied by an aquarium pump attached by PVC tube, (F) Pasture pipette, (G) scissor Jack, and (H) power supply.	39
Figure 3.1	Scanning electron microscopic photographs of (a) CS flakes, and (b) immobilized CS layer before the adsorption of RR4 dye (10,000x).	63

Figure 3.2	Scanning electron microscopic photographs of immobilized CS layer interface at (a) $0.65 \text{ mg cm}^{-2}$ , (b) $1.97 \text{ mg cm}^{-2}$ , and (c) $3.27 \text{ mg cm}^{-2}$ of CS loading.	64
Figure 3.3	FTIR spectra for (a) CS flake, (b) soluble CS layer, (c) semi-soluble CS layer, and (d) RR4-loaded CS layer.	67
Figure 3.4	Strength test of CS/glass at different CS loadings.	68
Figure 3.5	The effect of CS loading on the amount adsorbed and percentage of RR4 uptake at ambient pH (pH: 7.8) with initial dye concentration of $15 \text{ mg L}^{-1}$ and contact time of 2 h.	70
Figure 3.6	The effect of initial pH on the adsorption of RR4 by protonated and un-protonated CS/glass with CS loading of $0.65 \text{ mg cm}^{-2}$ , initial dye concentration of $15 \text{ mg L}^{-1}$ and contact time of 2 h.	72
Figure 3.7	The effects of initial dye concentration on the contact time and the amount of RR4 adsorbed by CS/glass with CS loading of $0.65 \text{ mg cm}^{-2}$ and initial pH of 6.0.	74
Figure 3.8	Pseudo-first-order kinetic model plots for the adsorption of RR4 by CS/glass at different initial dye concentrations with CS loading of $0.65 \text{ mg cm}^{-2}$ and initial pH of 6.0.	76
Figure 3.9	Pseudo-second-order kinetic model plots for the adsorption of RR4 by CS/glass at different initial dye concentrations with CS loading of $0.65 \text{ mg cm}^{-2}$ and initial pH of 6.0.	78
Figure 3.10	Intraparticle diffusion model plots for the adsorption of RR4 by CS/glass at different initial dye concentrations with CS loading of $0.65 \text{ mg cm}^{-2}$ and initial pH of 6.0.	80
Figure 3.11	Adsorption equilibrium of RR4 by air-dried and oven-dried CS/glass at different initial dye concentrations with CS loading of $0.65 \text{ mg cm}^{-2}$ , initial pH of 6.0 and contact time of 2 h.	82
Figure 3.12	Langmuir plot for the adsorption of RR4 by air-dried CS/glass at different initial dye concentrations with CS loading of $0.65 \text{ mg cm}^{-2}$ , initial pH of 6.0 and contact time of 2 h.	84

Figure 3.13	Langmuir plot for the adsorption of RR4 by oven-dried CS/glass at different initial dye concentrations with CS loading of $0.65 \text{ mg cm}^{-2}$ , initial pH of 6.0 and contact time of 2 h.	84
Figure 3.14	Freundlich plot for the adsorption of RR4 by air-dried CS/glass at different initial dye concentrations with CS loading of $0.65 \text{ mg cm}^{-2}$ , initial pH of 6.0 and contact time of 2 h.	88
Figure 3.15	Freundlich plot for the adsorption of RR4 by oven-dried CS/glass at different initial dye concentrations with CS loading of $0.65 \text{ mg cm}^{-2}$ , initial pH of 6.0 and contact time of 2 h.	88
Figure 3.16	Van't Hoff plot for the adsorption of RR4 by CS/glass at initial dye concentration of $40 \text{ mg L}^{-1}$ with CS loading of $0.65 \text{ mg cm}^{-2}$ , initial pH of 6.0 and contact time of 2 h.	91
Figure 4.1	UV-Vis DRS spectra of $50 \text{ mg L}^{-1}$ RR4 dye in ultra-pure water at ambient pH.	94
Figure 4.2	Cyclic voltammogram of 2.5% w/v RR4 in 0.1 M phosphate buffer pH 7.4.	95
Figure 4.3	UV-Vis DRS spectra of $\text{TiO}_2/\text{glass}$ , $\text{TiO}_2/\text{CS}/\text{glass}$ and $\text{TiO}_2/\text{RR4-CS}/\text{glass}$ systems.	98
Figure 4.4	PL spectra of $\text{TiO}_2/\text{glass}$ , $\text{TiO}_2/\text{CS}/\text{glass}$ and $\text{TiO}_2/\text{RR4-CS}/\text{glass}$ systems (Excitation wavelength = 325 nm).	98
Figure 4.5	TOC ( $\text{mg L}^{-1}$ ) values of irradiated water samples representing the leachability of organic matters from $\text{TiO}_2$ , $\text{TiO}_2/\text{CS}$ and $\text{TiO}_2/\text{RR4-CS}$ layers during repeated cycles of irradiation.	101
Figure 4.6	Spectral changes of RR4 dye within the $\text{TiO}_2/\text{RR4-CS}$ layered system monitored by UV-Vis DRS spectroscopy after each cycle of irradiation (each cycle is equivalent to 2 h of irradiation) in ultra-pure water.	103
Figure 4.7	Scanning electron microscopic photographs of $\text{TiO}_2$ layer interface at (a) 0.33, (b) 0.98, and (c) $1.64 \text{ mg cm}^{-2}$ of $\text{TiO}_2$ loading.	105

Figure 4.8	Effect of TiO <sub>2</sub> loading on the photocatalytic degradation of phenol by TiO <sub>2</sub> /RR4-CS/glass system at ambient pH (pH: 6.6) with initial phenol concentration of 10 mg L <sup>-1</sup> and aeration rate of 200 mL min <sup>-1</sup> .	107
Figure 4.9	UV-Vis DRS spectra of (a) un-irradiated CS/glass and irradiated CS/glass at (b) 0.33, (c) 0.98, (d) 1.30, (e) 2.29 and (f) 3.27 mg cm <sup>-2</sup> of TiO <sub>2</sub> loading in the TiO <sub>2</sub> /CS layered system for five cycles (10 h) in ultra-pure water.	111
Figure 4.10	The effect of aeration flow rate on the photocatalytic degradation of phenol by TiO <sub>2</sub> /RR4-CS layered system at ambient pH (pH: 6.6) with TiO <sub>2</sub> loading of 0.98 mg cm <sup>-2</sup> and initial phenol concentration of 10 mg L <sup>-1</sup> .	113
Figure 4.11	Scanning electron microscopic photographs of the TiO <sub>2</sub> top layer of (a) un-irradiated, and irradiated TiO <sub>2</sub> /CS layered system for the (b) third and (c) fifth cycles of irradiation in 20 mL of ultra-pure water (5,000x).	115
Figure 4.12	Amounts of RR4 adsorbed by un-irradiated and irradiated TiO <sub>2</sub> /CS layered system for one and five cycles at ambient pH (pH: 7.8) with initial RR4 concentration of 15 mg L <sup>-1</sup> and TiO <sub>2</sub> loading of 1.30 mg cm <sup>-2</sup> .	117
Figure 4.13	UV-Vis DRS spectra of chemisorbed RR4 dye in the CS sub-layer of (a) control plate, (b) un-irradiated and irradiated TiO <sub>2</sub> /CS layered system for the (c) one and (d) fifth cycles after 4 h of irradiation in ultra-pure water.	119
Figure 4.14	The effects of un-irradiated and irradiated TiO <sub>2</sub> /RR4-CS layered system on the photocatalytic degradation of phenol at ambient pH (pH: 6.6) with TiO <sub>2</sub> loading of 0.98 mg cm <sup>-2</sup> and initial phenol concentration of 10 mg L <sup>-1</sup> .	121
Figure 4.15	Percentages of RR4 remained after treatment by the TiO <sub>2</sub> /CS-ECH/glass and TiO <sub>2</sub> /CS-GLA/glass systems under dark and irradiated conditions at pH 4.0 with initial RR4 concentration of 15 mg L <sup>-1</sup> and TiO <sub>2</sub> loading of 0.33 mg cm <sup>-2</sup> .	124
Figure 4.16	PL spectra of TiO <sub>2</sub> /CS/glass, TiO <sub>2</sub> /CS-ECH/glass and TiO <sub>2</sub> /CS-GLA/glass systems (Excitation wavelength = 325 nm).	126



Figure 4.17	Reusability of immobilized TiO <sub>2</sub> /CS-ECH/glass and TiO <sub>2</sub> /CS-GLA/glass systems on the removal of RR4 under dark and irradiated conditions with initial RR4 concentration of 15 mg L <sup>-1</sup> and TiO <sub>2</sub> loading of 0.33 mg cm <sup>-2</sup> .	128
Figure 4.18	Percentages of RR4 remained after treatment by the TiO <sub>2</sub> /CS-GLA/glass system under dark and irradiated conditions at pH 3.0 with initial RR4 concentration of 15 mg L <sup>-1</sup> and TiO <sub>2</sub> loading of 0.33 mg cm <sup>-2</sup> .	129
Figure 4.19	Reusability of TiO <sub>2</sub> /CS-GLA/glass system on RR4 removal under irradiated condition at pH 3.0 with initial RR4 concentration of 15 mg L <sup>-1</sup> and TiO <sub>2</sub> loading of 0.33 mg cm <sup>-2</sup> .	129
Figure 5.1	Control experiments for the photocatalytic degradation of phenol by TiO <sub>2</sub> /glass, TiO <sub>2</sub> /CS/glass and TiO <sub>2</sub> /RR4-CS/glass systems at ambient pH (pH: 6.6) with TiO <sub>2</sub> loading of 0.98 mg cm <sup>-2</sup> and initial phenol concentration of 10 mg L <sup>-1</sup> .	132
Figure 5.2	Plot of ln(C <sub>0</sub> /C <sub>t</sub> ) versus time for the photocatalytic degradation of phenol by (a) TiO <sub>2</sub> /glass, (b) TiO <sub>2</sub> /CS/glass, and (c) TiO <sub>2</sub> /RR4-CS/glass systems.	133
Figure 5.3	The effect of initial pH on the photocatalytic degradation of phenol by TiO <sub>2</sub> /RR4-CS layered system with TiO <sub>2</sub> loading of 0.98 mg cm <sup>-2</sup> and initial phenol concentration of 10 mg L <sup>-1</sup> .	135
Figure 5.4	The effect of initial phenol concentration on the photocatalytic degradation of phenol by TiO <sub>2</sub> /RR4-CS layered system at ambient pH (pH: 6.6) with phenol concentrations of (a) 5 mg L <sup>-1</sup> , (b) 10 mg L <sup>-1</sup> , and (c) 20 mg L <sup>-1</sup> , and TiO <sub>2</sub> loading of 0.98 mg cm <sup>-2</sup> .	138
Figure 5.5	Percentage of phenol remained after photocatalytic reaction by the TiO <sub>2</sub> /RR4-CS layered system under different conditions at ambient pH (pH: 6.6) with TiO <sub>2</sub> loading of 0.98 mg cm <sup>-2</sup> and initial phenol concentration of 10 mg L <sup>-1</sup> .	140
Figure 5.6	FL spectral changes of TA solution in the TiO <sub>2</sub> /glass, TiO <sub>2</sub> /CS/glass and TiO <sub>2</sub> /RR4-CS/glass systems after 2 h of irradiation time at pH 7.0 and TiO <sub>2</sub> loading of 0.98 mg cm <sup>-2</sup> (Excitation wavelength = 315 nm).	145

Figure 5.7	Illustration of the possible mechanisms involved during the photocatalytic degradation of phenol by TiO <sub>2</sub> /RR4-CS layered system: (i) direct photocatalytic degradation of phenol by the TiO <sub>2</sub> photocatalyst, and (ii) charge transfer from the oxidation of chemisorbed RR4 dye at the TiO <sub>2</sub> /RR4-CS interface to the conduction band of TiO <sub>2</sub> .	147
Figure 5.8	Reusability of the immobilized photocatalyst systems on the (a) percentage of phenol removed and (b) pseudo-first-order rate constant at ambient pH (pH: 6.6) with TiO <sub>2</sub> loading of 0.98 mg cm <sup>-2</sup> and initial phenol concentration of 10 mg L <sup>-1</sup> .	151
Figure 5.9	Reusability of the partially and fully saturated TiO <sub>2</sub> /RR4-CS layered system on the photocatalytic degradation of phenol at ambient pH (pH: 6.6) with TiO <sub>2</sub> loading of 0.98 mg cm <sup>-2</sup> and initial phenol concentration of 10 mg L <sup>-1</sup> .	153
Figure 5.10	Pseudo-first-order rate constant values by partially-saturated and re-treated TiO <sub>2</sub> /RR4-CS layered system for the photocatalytic degradation of phenol upon reusability at ambient pH (pH: 6.6) with TiO <sub>2</sub> loading of 0.98 mg cm <sup>-2</sup> and initial phenol concentration of 10 mg L <sup>-1</sup> .	156
Figure 5.11	Time courses of TOC during the photocatalytic degradation of 50 mL phenol solution by the immobilized photocatalyst systems at ambient pH (pH: 6.6) with TiO <sub>2</sub> loading of 0.98 mg cm <sup>-2</sup> and initial phenol concentration of 10 mg L <sup>-1</sup> .	158
Figure 5.12	HPLC chromatograms of degraded species from phenol at (a) 60 and (b) 120 minutes of reaction time by TiO <sub>2</sub> /glass system.	160
Figure 5.13	HPLC chromatograms of degraded species from phenol at (a) 60 and (b) 120 minutes of reaction time by TiO <sub>2</sub> /CS/glass system.	161
Figure 5.14	HPLC chromatograms of degraded species from phenol at (a) 60 and (b) 120 minutes of reaction time by TiO <sub>2</sub> /RR4-CS/glass system.	161
Figure 5.15	The time course of PhOH and its main intermediates detected by HPLC during the photocatalytic degradation of PhOH by TiO <sub>2</sub> /glass system.	163

Figure 5.16	The time course of PhOH and its main intermediates detected by HPLC during the photocatalytic degradation of PhOH by TiO <sub>2</sub> /CS/glass system.	163
Figure 5.17	The time course of PhOH and its main intermediates detected by HPLC during the photocatalytic degradation of PhOH by TiO <sub>2</sub> /RR4-CS/glass system.	164
Figure 5.18	The proposed degradation pathway for the photocatalytic degradation of phenol by the immobilized photocatalyst systems.	167

## LIST OF SYMBOLS AND ABBREVIATIONS

AOP	Advanced oxidation process
BET	Brunauer-Emmett-Teller
BJH	Barrett-Joyner-Halenda
BQ	1,4-benzoquinone
CAT	Catechol
CB	Conduction band
CS	Chitosan
CV	Cyclic voltammetry
DOM	Dissolved organic matter
DRS	Diffuse reflectance spectroscopy
$e^-$	Negatively charged electron
ECH	Epichlorohydrin
$E_g$	Band-gap energy
$E_{\text{HOMO/LUMO}}$	Energy levels of the HOMO and the LUMO
ENR <sub>50</sub>	Epoxidized natural rubber
FL	Fluorescence
FTIR	Fourier transform infrared
FUM	Fumaric acid
GLA	Glutaraldehyde
$h^+$	Positively charged hole
HOMO	Highest occupied molecular orbital
HPLC	High performance liquid chromatography
HQ	Hydroquinone

$h\nu$	Photonic energy
IC	Ion chromatography
$k$	Pseudo-first-order rate constant
LUMO	Lowest unoccupied molecular orbital
MAL	Maleic acid
NHE	Normal hydrogen electrode
PF	Phenol formaldehyde
PhOH	Phenol
PL	Photoluminescence
PVC	Polyvinyl chloride
$R^2$	Linear regression coefficient
RR4	Reactive Red 4
SEM	Scanning electron microscopy
TA	Terephthalic acid
TAOH	Hydroxyterephthalic acid
TOC	Total organic carbon
UV	Ultraviolet
VB	Valence band
Vis	Visible
$\lambda$	Wavelength (nm)

**SISTEM TERIMOBILISASI BERLAPISAN TiO<sub>2</sub>/KITOSAN  
MENGGABUNGKAN PEWARNA REAKTIF MERAH 4 UNTUK  
PENGURAIAN PEMFOTOMANGKIN FENOL**

**ABSTRAK**

Sistem terimobilisasi berlapisan TiO<sub>2</sub>/kitosan menggabungkan pewarna Reaktif Merah 4 (RR4) telah berjaya difabrikasikan, dioptimumkan, dan digunakan untuk penyingkiran fenol di bawah 45 W lampu pendarfluor padat. Fotomangkin terimobilisasi tersebut telah disediakan dengan menjerap pewarna RR4 di atas sub-lapisan kitosan (CS) yang disokong oleh plat kaca, sebelum disaluti oleh TiO<sub>2</sub> sebagai lapisan atas (dikenali sebagai TiO<sub>2</sub>/RR4-CS/kaca). Kajian terhadap penjerapan pewarna RR4 oleh sub-lapisan CS menunjukkan bahawa penjerapan RR4 yang tertinggi dicapai oleh CS/kaca adalah pada berat bebanan CS 0.65 mg cm<sup>-2</sup> (bersamaan dengan 6.15 ± 0.13 µm dalam ketebalan), dan pH 6.0 pada suhu bilik (300 K). CS/kaca berlapisan nipis adalah lebih bersesuaian dan efektif dalam menjerap RR4 jika dibandingkan dengan lapisan tebal kerana ia meningkatkan luas permukaan CS dan keliangannya. Model-model isoterma Langmuir dan Freundlich berkorelasi secara baik dengan data penjerapan dengan  $q_{max}$  bernilai 86.2 mg g<sup>-1</sup>, mencadangkan bahawa CS/kaca adalah mod yang sesuai digunakan sebagai penambat pewarna.

Apabila digabungkan dengan TiO<sub>2</sub> melalui susunan berlapisan, didapati bahawa berat bebanan TiO<sub>2</sub> yang optimum diperolehi ialah 0.98 mg cm<sup>-2</sup> (bersamaan dengan ketebalan 14.5 ± 0.41 µm). Berat bebanan mangkin yang melebihi nilai

optimum akan menghadkan pembauran molekul-molekul pencemar serta radikal-radikal oksidaan menuju ke antara muka  $\text{TiO}_2/\text{RR4-CS}$ , meningkatkan kesan penyerakan cahaya, meningkatkan perpaduan semula pasangan elektron-lubang dan menyebabkan pengoksidaan sub-lapisan CS. Punaran-foto ke atas sistem fotomangkin membolehkan plat-plat yang telah difabrikasi “dibersihkan” daripada penguraian pengikat-pengikat organik, larut lesap sub-lapisan CS dan fotopelunturan oleh pengkimierapan pewarna RR4. Tambahan pula, makroliang turut terbentuk di dalam lapisan atas  $\text{TiO}_2$ , yang meningkatkan penembusan cahaya dan membolehkan pembauran pencemar dengan lebih baik dan juga radikal-radikal oksidaan merentasi lapisan dalam  $\text{TiO}_2/\text{RR4-CS/kaca}$ .  $\text{TiO}_2/\text{RR4-CS}$  melalui sistem berlapisan mempamerkan kecekapan pemfotomangkinan yang tinggi untuk penguraian dan pemineralan fenol masing-masing dengan kadar penguraian  $0.030 \pm 0.000 \text{ min}^{-1}$  dan jumlah pemineralan  $76.7 \pm 0.0\%$ . Fotomangkin terubahsuai itu juga telah digunakan semula untuk sekurang-kurangnya lima kitaran penggunaan berpanjangan tanpa kehilangan kecekapannya. Mekanisme  $\text{TiO}_2/\text{RR4-CS}$  melalui sistem berlapisan menunjukkan pewarna itu sendiri tidak teruja oleh cahaya tetapi sebaliknya lubang yang terbentuk daripada pengujaan zarah  $\text{TiO}_2$  menghasilkan radikal  $\text{OH}^\bullet$  yang mengoksidakan anion-anion pewarna dan dengan demikian mengaruhkan suntikan elektron kepada jalur konduksi  $\text{TiO}_2$ . Elektron-elektron yang berlebihan di dalam jalur konduksi  $\text{TiO}_2$  telah memecutkan pemfotomangkin fenol.

# **IMMOBILIZED TiO<sub>2</sub>/CHITOSAN LAYERED SYSTEM INCORPORATING REACTIVE RED 4 DYE FOR THE PHOTOCATALYTIC DEGRADATION OF PHENOL**

## **ABSTRACT**

An immobilized TiO<sub>2</sub>/chitosan layered system incorporating Reactive Red 4 (RR4) dye has been successfully fabricated, optimized and applied for the removal of phenol under a 45 W compact fluorescent lamp. The immobilized photocatalyst was prepared by adsorbing RR4 dye on chitosan (CS) sub-layer supported by glass plate, before being coated by TiO<sub>2</sub> as the top layer (known as TiO<sub>2</sub>/RR4-CS/glass). Studies on the adsorption of RR4 dye by CS sub-layer showed that the highest RR4 uptake by CS/glass can be achieved at CS loading of 0.65 mg cm<sup>-2</sup> (corresponding to 6.15 ± 0.13 μm in thickness), and pH 6.0 under room temperature (300 K). Thinner layer of CS/glass is favorable and more effective in adsorbing RR4 compared to thicker layer as it increases the surface area and porosity of CS. Langmuir and Freundlich isotherm models correlated well with the adsorption data with  $q_{max}$  of 86.2 mg g<sup>-1</sup>, suggesting that CS/glass is a viable mode for anchoring the dye.

When combined with TiO<sub>2</sub> in a layered assemblage, it was found that the optimum loading of TiO<sub>2</sub> obtained was 0.98 mg cm<sup>-2</sup> (equivalent to 14.5 ± 0.41 μm of thickness). Catalyst loading higher than the optimum value limits the diffusion of pollutant molecules as well as oxidative radicals towards the TiO<sub>2</sub>/RR4-CS interface, increased the light scattering effect, enhanced the recombination of electron-hole pairs and caused the oxidation of CS sub-layer. Photo-etching of the photocatalyst



systems allowed the “cleaning” of the fabricated plates from the degradation of organic binders, leaching of CS sub-layer and photobleaching of chemisorbed RR4 dye. In addition, macro-pores were also generated within the TiO<sub>2</sub> top layer, which increased the light penetration and allowed better diffusion of the pollutant as well as oxidative radicals across the inner layer of the TiO<sub>2</sub>/RR4-CS/glass. The TiO<sub>2</sub>/RR4-CS layered system exhibited high photocatalytic efficiencies for the degradation and mineralization of phenol with degradation rate of  $0.030 \pm 0.000 \text{ min}^{-1}$  and total mineralization of  $76.7 \pm 0.0\%$ , respectively. The modified photocatalyst was also reusable for at least five cycles of extended usage without losing its efficiency. The mechanism of TiO<sub>2</sub>/RR4-CS layered system suggested that the dye itself was not excited by light but in fact, the holes generated from excitation of TiO<sub>2</sub> particle produced OH<sup>•</sup> radicals that oxidized the dye anions thus induced electron injection to the conduction band of TiO<sub>2</sub>. Excess electrons in the conduction band of TiO<sub>2</sub> accelerated the photocatalytic degradation of phenol.

## **CHAPTER ONE**

### **INTRODUCTION**

#### **1.1 Background**

Wastewater effluent from industries and household has become a major problem both in Malaysia and in other parts of the world. It has been estimated that Malaysia generates about six million tons of sewage every year (Liew, 2008). Most of these wastes will eventually end up in the surface water. Untreated wastewater has a variety of organic compounds with variable toxicity, carcinogenic and mutagenic properties. Many of them contain aromatic rings which are generally resistant to chemical, photochemical as well as biological degradation. They are persistent in the environment and have the potential to cause negative impacts to human health and the ecosystem. Therefore, it is very important to treat these pollutants and keeps its concentration below the acceptable limits before being discharged into the surface water.

Conventional methods of treating organic wastewater includes adsorption, sedimentation, coagulation and flocculation, filtration, biological treatments, chemical oxidation, ozonation, electrochemical and photolysis. These existing water treatment processes have been shown to be effective, but they have a number of limitations. Most of these conventional treatments and detoxification of wastewater are expensive, technically complicated, slow, ineffective and not environmentally compatible. Furthermore, excess amount of chemical usage and generation of

secondary waste can add to the disposal problems. For example, adsorption and coagulation techniques applied to treat organic pollutants in wastewater are non-destructive processes, which mean that the pollutants will not be degraded. In this case, the pollutants are concentrated and transferred from water to another phase leading to the generation of secondary waste (Konstantinou and Albanis, 2004). In biological treatments, extreme experimental conditions as well as the toxicity of the target pollutants and its intermediates can be lethal for the microorganisms intended to degrade them (Ray, 1999). Because of the problems associated with the practical applications of these techniques especially in removing trace amounts of impurities, many of the methods used for treating organics in wastewater have not been widely applied on a large scale.

## **1.2 Photocatalysis**

### **1.2.1 Definition**

The initial interest in photocatalysis was generated by the discovery of “Honda-Fujishima Effect” in the early 1970s (Fujishima and Honda, 1972). This study involves the photoelectrochemical water splitting using a single-crystal titania electrode, which is related to photocatalysis. Since then, tremendous level of interest in photocatalysis has been shown by researchers all over the world which was reflected by an increasing number of articles published over the years (Figure 1.1). An overview of the many possibilities of photocatalysis is given in recent reviews (Fujishima *et al.*, 2007; Palmisano *et al.*, 2010; Di Paola *et al.*, 2012). This technology has been successfully applied to water splitting and hydrogen production,

photodestruction of bacteria and cancer cells, self-cleaning, organic synthesis as well as environmental remediation for air and water purification.

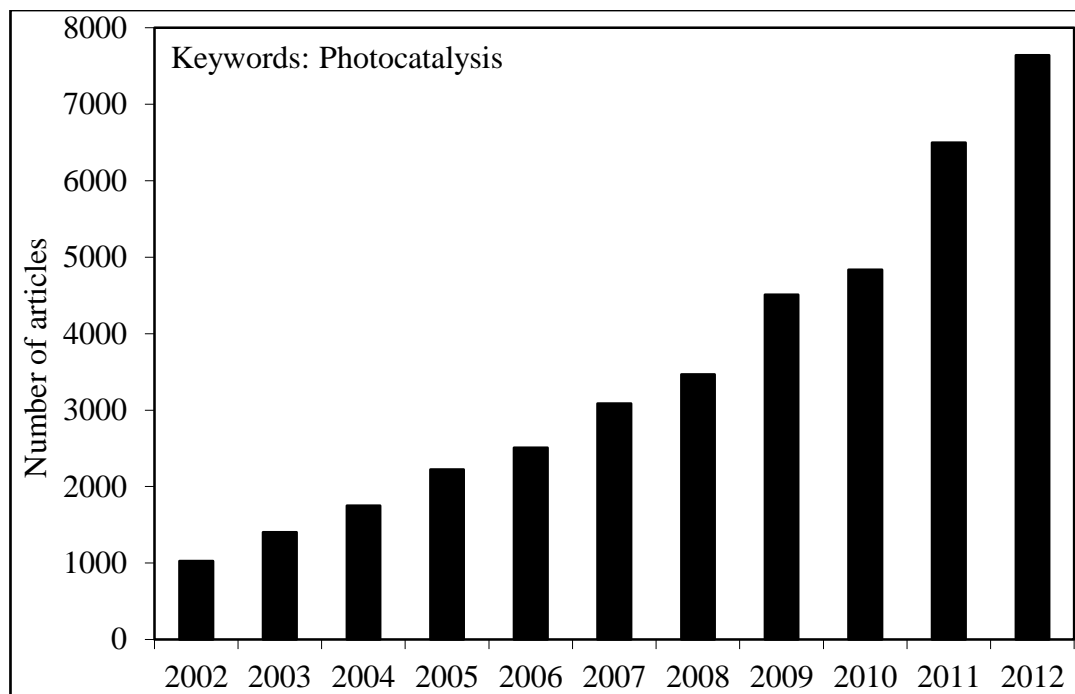


Figure 1.1: A Scopus database literature survey of research articles published on photocatalysis from 2002 to 2012 (the survey does not include patents).

The term “photocatalysis” generally means the acceleration of a photoreaction by the presence of a catalyst (Mills and Le Hunte, 1997). The photoreactions is characterized by the free radical mechanism initiated by the absorption of a photon with sufficient energy, i.e., equal or higher than the band-gap energy of the catalyst. As one of the advanced oxidation processes (AOP), heterogeneous photocatalysis is more favorable in wastewater treatment for the degradation and mineralization of different types of toxic pollutants as compared to homogeneous system. This is because the photoreactions occur at the surface of a catalyst rather than in the bulk solution (Mills and Le Hunte, 1997). Hence it would be much easier to remove the photocatalysts from the reaction solution. Besides,

heterogeneous photocatalysis has many benefits over other conventional treatments for the detoxification of wastewater such as (Gogate and Pandit, 2004; Gupta and Tripathi, 2011; McCullagh *et al.*, 2011):

- 1) Complete mineralization of organic pollutants (such as polymers, dyes, surfactants, pesticides and herbicides) to yield CO<sub>2</sub>, H<sub>2</sub>O and mineral acids.
- 2) It does not produce secondary pollutants and/or generate waste.
- 3) It does not require the use of hazardous chemicals or materials such as hypochlorite, peroxide or ozone. Hence, less input of chemicals is needed during the photoreactions.
- 4) The possibility to effectively use sunlight or near UV light for irradiation can result in considerable economic savings especially for large-scale operations. In fact, the photocatalysts used in the photoreactions are usually inexpensive.
- 5) The photoreactions conditions only need mild temperature and pressure conditions with modest reaction time.
- 6) The generated intermediates of treated hazardous compounds are minimal.
- 7) Potential applications in gaseous phase and solid phase treatments.

### **1.2.2 Principles of a heterogeneous photocatalysis**

Heterogeneous photocatalytic reaction can only occur in the presence of three basic components: an emitted photon (in the appropriate wavelength), a strong oxidizing agent (usually oxygen), and a catalyst surface (a semiconductor material) (Teh and Mohamed, 2011). It uses a continuously illuminated, photoexcitable solid catalyst or semiconductor photocatalyst to accelerate photoreaction as well as to

convert persistent organic pollutants to a more biologically degradable and less toxic substances. A semiconductor is a material with electric resistivity between that of an insulator and a conductor and is usually characterized by an electronic band structure in which the highest occupied energy band, called valence band (VB), and the lowest empty band, called conduction band (CB), are separated by a band-gap, i.e. a region of forbidden energies in a perfect crystal (Teh and Mohamed, 2011).

The principles of photocatalytic oxidation have been reviewed extensively (Hoffmann *et al.*, 1995; Litter, 1999). Generally, when a photon of energy higher or equal to the band-gap energy is absorbed by a semiconductor particle, an electron ( $e^-$ ) from the VB is promoted to the CB with the simultaneous generation of a positive hole ( $h^+$ ) in the VB (Figure 1.2). The  $e^-$  and the  $h^+$  can recombine on the surface or in the bulk of the particle (and the energy dissipated as heat) or can be trapped in surface states where they can react with electron donors (such as organic molecules or  $OH^-$  groups) or electron acceptors (such as oxygen molecules or  $H^+$ ) adsorbed or close to the surface of the particle. Hence, subsequent anodic and cathodic redox reactions can be initiated.

The energy level at the bottom of the CB is actually the reduction potential of photoelectrons and the energy level at the top of the VB determines the oxidizing ability of photoholes. Each value of the energy level reflect the ability of the system to promote reductions and oxidations (Litter, 1999). The efficiency of a semiconductor photocatalyst actually depends on the competition of different interface transfer processes involving  $e^-$  and  $h^+$  as well as their deactivation by recombination.

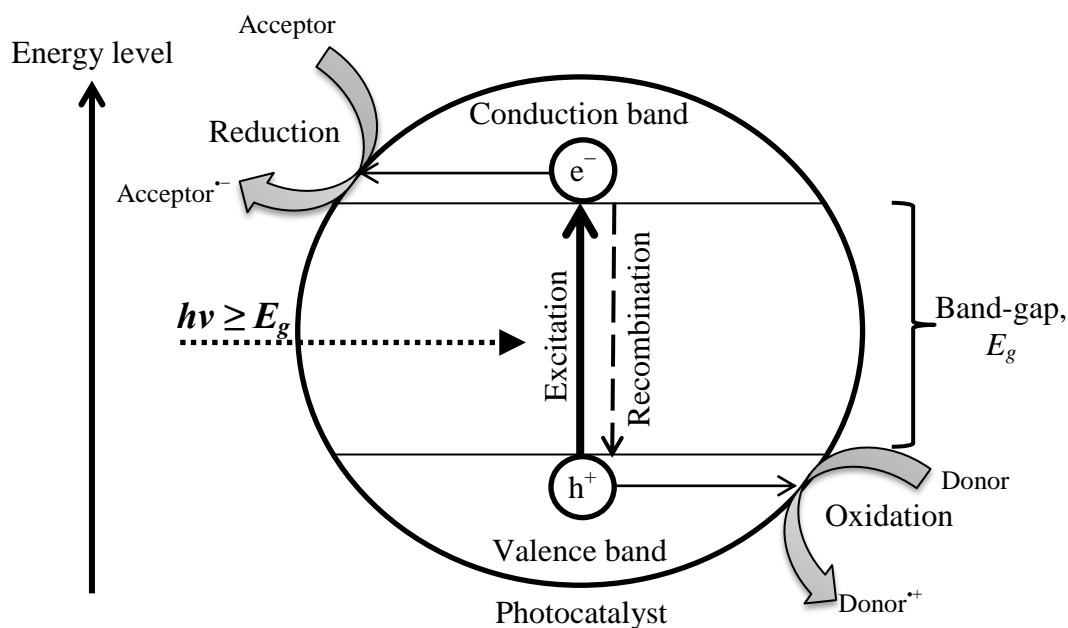


Figure 1.2: Schematic illustration of the photoinduced hole and electron over photon activated semiconductor photocatalyst.

Various semiconductors with different band-gap energies such as  $\text{TiO}_2$ ,  $\text{ZnO}$ ,  $\text{GaP}$ ,  $\text{CdS}$ , etc. have been used as photocatalysts in the literatures (Figure 1.3). They are used in photocatalysis because of a favorable combination of electronic structure, light absorption properties, charge transport characteristics, and excited-state lifetimes (Thiruvengkatachari *et al.*, 2008). The surface area and the number of active sites offered by the photocatalyst (thus the nature of the photocatalyst, i. e. crystalline or amorphous is important) for the adsorption of pollutants, plays an important role in deciding the overall rates of degradation (Xu *et al.*, 1999; Gogate and Pandit, 2004).

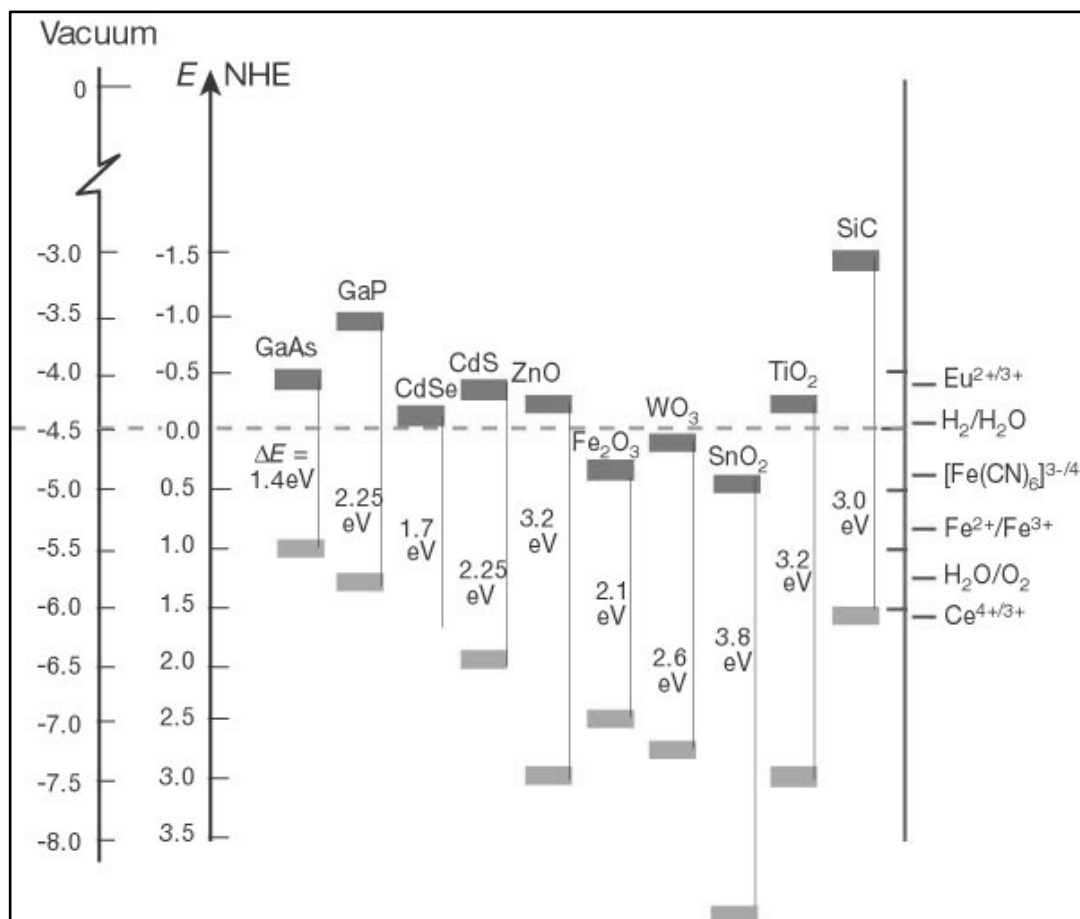


Figure 1.3: Band positions of several semiconductors in contact with aqueous electrolyte at pH 1 (Gratzel, 2001).

### 1.3 Titanium dioxide ( $TiO_2$ )

#### 1.3.1 General

Titanium dioxide ( $TiO_2$ ) is a transition metal oxide which is a natural occurring form of titanium. It is also known as titania or titanium (IV) oxide. As a n-type semiconductor,  $TiO_2$  is chemically and biologically inert, photocatalytically and thermally stable, high photoconductivity, relatively easy to produce and to use. It has long durability, and is cheap and safe toward both human as well as the environment. Due to these unique characteristics,  $TiO_2$  has been successfully applied in



widespread applications such as paints, papers, sunscreens, cosmetics, anti-fogging and self-cleaning surfaces, food and pharmaceutical additive, air and water purification systems, sterilization, water splitting and hydrogen production, and photoelectrochemical conversion (Carp *et al.*, 2004; Fujishima *et al.*, 2008; Gupta and Tripathi, 2011).

### 1.3.2 Properties of TiO<sub>2</sub> semiconductor

The crystalline structure of TiO<sub>2</sub> has been reported as one of the factors affecting its performance. As shown in Figure 1.4, there are three commonly known polymorphs of TiO<sub>2</sub> found in nature (Gupta and Tripathi, 2011):

- 1) Rutile: It has a tetragonal structure with 6 atoms per unit cell and the TiO<sub>6</sub> octahedron is slightly distorted. It is the most stable and common form of TiO<sub>2</sub> at most temperatures and pressures.
- 2) Anatase: It also has a tetragonal structure but the distortion of the TiO<sub>6</sub> octahedron is slightly larger than the rutile phase.
- 3) Brookite: It belongs to the orthorhombic crystal system in which its unit cell is composed of 8 formula units of TiO<sub>2</sub> and is formed by edge-sharing TiO<sub>6</sub> octahedral.

Upon heating at high temperature, the anatase and brookite forms of TiO<sub>2</sub> tend to convert into rutile form (Teh and Mohamed, 2011). However, the performance of the rutile phase as a photocatalyst is generally very poor (Gupta and Tripathi, 2011).

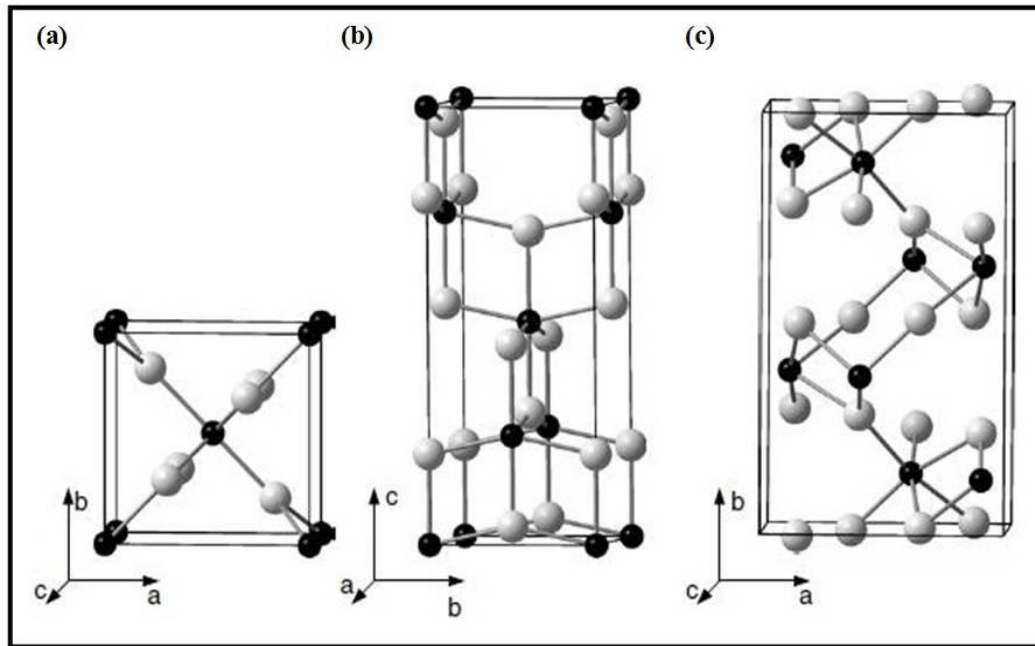


Figure 1.4: Bulk crystalline structures of the (a) rutile, (b) anatase, and (c) brookite type  $\text{TiO}_2$  (Janisch *et al.*, 2005).

Generally, the anatase phase is preferred over other polymorphs for the photocatalytic application because of its higher electron mobility, low dielectric constant, lower density, slightly higher Fermi level, lower capacity to adsorb oxygen and higher degree of hydroxylation as compared to the rutile phase (Tanaka *et al.*, 1991; Gupta and Tripathi, 2011). Meanwhile, brookite  $\text{TiO}_2$  is not often used for experimental investigations due to its much more complicated crystalline structure.

$\text{TiO}_2$  absorbs radiation below the visible range of light spectrum due to its wide band-gap energy. It requires radiation of wavelength  $300 \text{ nm} < \lambda < 380 \text{ nm}$  for a photoreaction to occur. Consequently, the photoactivation of  $\text{TiO}_2$  can be achieved by irradiation with artificial lamps (such as compact fluorescent lamp or low-pressure mercury lamp) or by solar irradiation.

### 1.3.3 TiO<sub>2</sub> in photocatalysis

TiO<sub>2</sub> is considered to be a benchmark semiconductor for photocatalysis because it is the most efficient and photocatalytically active photocatalyst as compared to other semiconductors. Its strong oxidizing agent, such as hydroxyl radical, is capable of degrading organic pollutants (such as dyes, polymers, pesticides, herbicides, etc.) present at or near the surface of the TiO<sub>2</sub> resulting usually in their complete mineralization into H<sub>2</sub>O and CO<sub>2</sub> by irradiation with UV light. Other photocatalysts reported in the literature possess limitation. For example, CdS is not sufficiently stable for catalysis in aqueous media as it readily undergoes photocorrosion and is also toxic (Mills and Le Hunte, 1997; Gupta and Tripathi, 2011). ZnO is unstable because it readily dissolves in water to yield Zn(OH)<sub>2</sub> on the ZnO particle surface, which inactivates the catalyst over time (Bahnemann *et al.*, 1987; Gupta and Tripathi, 2011).

The photoreaction of TiO<sub>2</sub> is derived from the formation of photoinduced hole and electron after the absorption of photon energy corresponding to the band-gap energy of TiO<sub>2</sub> ( $\lambda < 380$  nm). The photoinduced holes in the valence band diffuse to the surface of TiO<sub>2</sub> and react with adsorbed water molecules or hydroxide ions (OH<sup>-</sup>) in aqueous solution and produce hydroxyl radicals (OH<sup>•</sup>). Meanwhile, electrons in the conduction band typically participate in reduction processes, which react with dissolved oxygen molecules to produce various species such as superoxide radicals (O<sub>2</sub><sup>•-</sup>), hydroperoxyl radicals (HOO<sup>•</sup>), hydrogen peroxide (H<sub>2</sub>O<sub>2</sub>), and OH<sup>•</sup> radicals. Such oxygen-containing species can be photocatalytically very active in the mineralization of organic contaminants. The overall mechanism of photoinduced

hole and electron as well as the oxidative-reductive reactions that take place at the photoinduced  $\text{TiO}_2$  surface when it is irradiated with adequate  $h\nu$  is depicted in Figure 1.5. The main pathway of organic compounds by  $\text{TiO}_2$  photocatalytic system could be summarized by the following reaction:

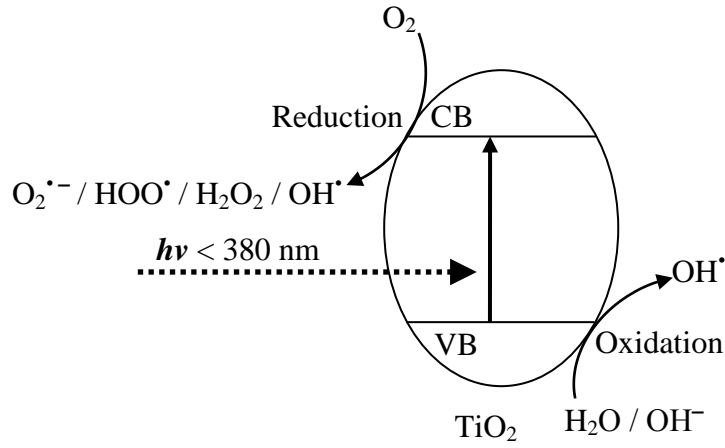
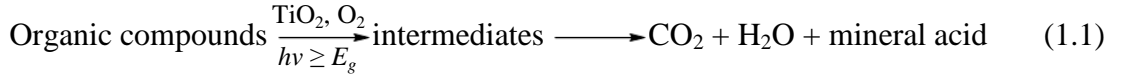


Figure 1.5: Mechanism of photoinduced hole and electron on the surface of  $\text{TiO}_2$  photocatalyst.

#### 1.3.4 Drawbacks of $\text{TiO}_2$ photocatalyst

Despite its advantages, the crucial obstacles of using  $\text{TiO}_2$  semiconductor in photocatalytic reactors can be listed as follows (Bhattacharyya *et al.*, 2004; Qu, 2008; Thakur *et al.*, 2010; Teh and Mohamed, 2011):

- 1) The regeneration, recovery and reuse of  $\text{TiO}_2$  are a problem. This is because the use of  $\text{TiO}_2$  in a slurry or suspension mode would require a post-treatment to recover the catalyst from the water which can be difficult, time consuming

and expensive. Moreover, the fine  $\text{TiO}_2$  particles have a great tendency to aggregate which provides a real limitation to be applied to a continuous flow system. Furthermore, the slurry system normally suffers from light scattering effect by the suspended particles.

- 2) The photocatalytic reaction by  $\text{TiO}_2$  photocatalyst is relatively slow due to its low adsorption ability especially for non-polar organic compounds, due to its polar surface, that limits its degradation efficiencies to only selective compounds.
- 3) High recombination rate of photoinduced electron-hole pairs results in process inefficiencies and waste of the energy supplied by the photon.
- 4)  $\text{TiO}_2$  has a large band gap energy ( $\sim 3.2$  eV) and thus adsorbs only a small portion (5 – 7%) of solar spectrum in the UV region leading to a low degradation rate and quantum efficiency. Besides, the use of high-energy UV light or strong oxidants can cause serious hazard to human being and expensive in term of cost.

These drawbacks restrict the large-scale applications of  $\text{TiO}_2$ . Hence, the modification of  $\text{TiO}_2$  is necessary in order to improve its photocatalytic performances.

#### **1.4 Modification of $\text{TiO}_2$**

Numerous approaches have been conducted in order to enhance the photocatalytic efficiency of  $\text{TiO}_2$ . This can be achieved by either morphological modification, such as increasing surface area and porosity, or chemical modification

that is by the incorporation of additional components in the TiO<sub>2</sub> structure in order to shift the response and increase the sensitivity of TiO<sub>2</sub> towards the visible light region and/or to increase the lifetime of the photoinduced electron-hole pairs (Pelaez *et al.*, 2012). Some of the techniques used to modify TiO<sub>2</sub> includes immobilization (Mascolo *et al.*, 2007; Caballero *et al.*, 2009; Nawi *et al.*, 2011b; Wong *et al.*, 2011; Nawi and Zain, 2012), combination with adsorbent (El-Sharkawy *et al.*, 2007; Li *et al.*, 2008; Zainal *et al.*, 2009; Miller and Zimmerman, 2010; Brigante and Schulz, 2011; Nawi *et al.*, 2012b), dye-modification (Hilal *et al.*, 2007; Kaur and Singh, 2007; Kuo *et al.*, 2008; Vinu *et al.*, 2010; Qin *et al.*, 2011), doping with metal (Janisch *et al.*, 2005; Teh and Mohamed, 2011) and non-metal (Chen *et al.*, 2009; Joshi *et al.*, 2009; Kim *et al.*, 2011; Teh and Mohamed, 2011; Mangrulkar *et al.*, 2012), as well as coupling of semiconductor (Chen *et al.*, 2011b; Ku *et al.*, 2011; Su *et al.*, 2011; Zhu *et al.*, 2012). Modifications of TiO<sub>2</sub> by immobilization on solid support, combination with adsorbent and dye-modified are further discussed in the following sections. These techniques are considered to be the easiest, cost-effective and most efficient methods to modify TiO<sub>2</sub>.

#### **1.4.1 Immobilization of TiO<sub>2</sub>**

Photocatalysis with TiO<sub>2</sub> powder uses two kinds of reaction systems, namely (1) TiO<sub>2</sub> suspended in aqueous medium and (2) TiO<sub>2</sub> immobilized on support materials. Suspended TiO<sub>2</sub> have higher photocatalytic efficiency than in immobilized form because of their higher specific surface area. However, the separation of suspension from the liquid state used in water treatment and recycling processes is troublesome because of the formation of aggregates. In addition, the depth of

penetration of UV light is limited because of the strong absorption by both catalyst particles and dissolved organic species (Thiruvengkatachari *et al.*, 2008). Immobilization of TiO<sub>2</sub> powder on solid supports is an alternative and convenient method to solve the problem of the post-treatment catalyst powder recovery and facilitate the photocatalyst usage for long-term applications. In addition, there is a possibility of better reactions control which can be easily adapted into different kinds of designs such as column, rod, etc. Hence, more favorable economic factors can be expected. TiO<sub>2</sub> may be immobilized on suitable solid support matrix such as glass, quartz, sand, membrane, silica, ceramics, activated carbon, zeolites, glass fibers or stainless steel. These can eliminate the problem of agglomeration and the need for post-treatment removal of the used catalyst. In fact, it also allows the recovery and continuous reuse of the TiO<sub>2</sub> photocatalyst.

However, unfortunately, the surface area available for the reaction decreases due to the fixing of the catalyst on the solid supports as well as low porosity of the supported catalyst layer and this in turn lowers the photocatalytic efficiencies of the immobilized TiO<sub>2</sub> (Guillard *et al.*, 2003; Mascolo *et al.*, 2007). Furthermore, the catalyst must adhere to the solid support substrate in the reactor and, unless the substrate is UV transparent, the reactor design is limited by the optical constraints (An *et al.*, 2006). Besides, the problem of scouring or detachment of the deposited catalyst particles, a part of the porous structure of TiO<sub>2</sub> gets lost during the heating process and also the difficulty to support powdered TiO<sub>2</sub> on some materials reduces the photocatalytic efficiency of the immobilized TiO<sub>2</sub> (Bideau *et al.*, 1995; Thiruvengkatachari *et al.*, 2008).

### 1.4.2 Combination with adsorbents

Combining  $\text{TiO}_2$  with adsorbent such as activated carbon (El-Sharkawy *et al.*, 2007; Zhang *et al.*, 2011), silica (Zhang *et al.*, 2009b; Brigante and Schulz, 2011), zeolites (Bhattacharyya *et al.*, 2004; Shankar *et al.*, 2006) or chitosan (Zubieta *et al.*, 2008; Zainal *et al.*, 2009; Nawi *et al.*, 2010) would be of great interest. The adsorbent not only offer a support for the  $\text{TiO}_2$ , but would also provide higher specific surface area and facilitate more effective adsorption than bare  $\text{TiO}_2$  as it concentrates the pollutants and intermediates around the surface of  $\text{TiO}_2$  where they would be degraded (Bhattacharyya *et al.*, 2004; Zhang *et al.*, 2011). The photocatalytic reactions of the system, hence, will be improved due to the synergistic effect of adsorption and photocatalysis processes. For example, Araña *et al.* (2003) reported that powdered activated carbon (PAC) can be very efficient when it is mixed with  $\text{TiO}_2$  in photocatalytic processes. They observed that (1) the combination of PAC and  $\text{TiO}_2$  results in fast decantability in comparison with that of  $\text{TiO}_2$  alone, (2) a  $\text{TiO}_2$  particle distribution on the PAC surface yields a homogeneous particle size distribution, and (3) the rate of organic removal by the PAC and  $\text{TiO}_2$  was six times higher than that with  $\text{TiO}_2$  alone. However, most of the conducted studies have physically or chemically mixed the adsorbent with the photocatalyst, either of which could limit the performance of adsorbent or the photocatalyst.

### 1.4.3 Dye-modified $\text{TiO}_2$

Modification of  $\text{TiO}_2$  with dye is an interesting research area as dye is capable of adsorbing visible light as a photosensitizer for transferring energy to  $\text{TiO}_2$



or  $O_2$ , making the reaction mixture more sensitive to light, and therefore promoting the degradation efficiency of pollutants (Kuo *et al.*, 2008). In fact, dye-modified  $TiO_2$  has received much attention in photovoltaic applications, such as dye-sensitized cells (Nazeeruddin *et al.*, 1993; Islam *et al.*, 2001; Sharma *et al.*, 2010) and photolysis of water to generate hydrogen (Jin *et al.*, 2007; Li *et al.*, 2009). An excellent review regarding this subject matter has recently been published (Rehman *et al.*, 2009; Gupta and Tripathi, 2011; Kumar and Devi, 2011; Pei and Luan, 2012). The incorporation of dye in the  $TiO_2$  photocatalytic system has been reported to be the most effective way to extend the photoresponse of  $TiO_2$  into the visible region. In such technique, the dye is anchored on the surface of the photocatalyst by either covalent bonding, ion-pair type association, physisorption, entrapment in cavities or pores and hydrophobic interactions leading to self-assembly of monolayers (Kalyanasundaram and Grätzel, 1998; Chatterjee and Dasgupta, 2005). The interaction between the dye and  $TiO_2$  increases the efficiency of the excitation process and expands the wavelength response of the photocatalyst (Gupta and Tripathi, 2011).

Generally, the mechanism of the dye-sensitized photodegradation of pollutants (shown in Figure 1.6) is based on the absorption of visible light for exciting an electron from the highest occupied molecular orbital (HOMO) to the lowest unoccupied molecular orbital (LUMO) of a dye. The excited dye molecule subsequently transfers electrons into the conduction band of  $TiO_2$ , while the dye itself is converted to its cationic radical. The  $TiO_2$  acts only as a mediator for transferring electrons from the sensitizer to the substrate on the  $TiO_2$  surface as electron acceptors, and the valence band of  $TiO_2$  remains unaffected. In this process,

the LUMO of the dye molecules should be more negative than the conduction band of  $\text{TiO}_2$ . The injected electrons hop over quickly to the surface of  $\text{TiO}_2$  where they are scavenged by molecular oxygen to form superoxide radicals ( $\text{O}_2^{\cdot-}$ ), hydroperoxyl radicals ( $\text{HOO}^{\cdot}$ ), hydrogen peroxide ( $\text{H}_2\text{O}_2$ ) and hydroxyl radicals ( $\text{OH}^{\cdot}$ ). In addition, singlet oxygen may also be formed under certain experimental conditions (Pelaez *et al.*, 2012).

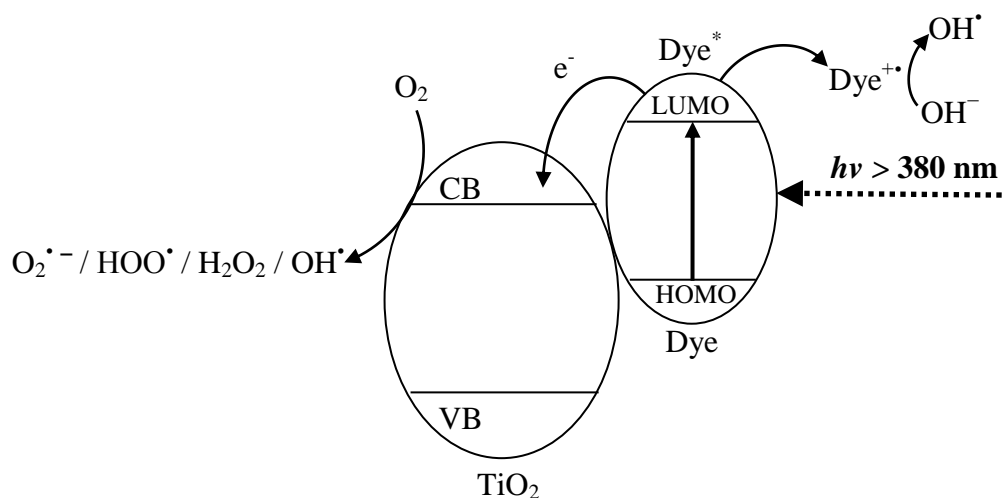


Figure 1.6: Mechanism of the dye-sensitized  $\text{TiO}_2$  photocatalyst.

The electron injection and back electron-transfer rates from the dye to the photocatalyst depend upon the nature of the dye molecules, properties of the  $\text{TiO}_2$  and the interactions between the dye and  $\text{TiO}_2$  (Gupta and Tripathi, 2011). However, even though the dye may give an increase in visible light absorption in  $\text{TiO}_2$ , it does not guarantee visible light induced activity. This is because only few dyes can provide a high photocurrent quantum yield. In this case, other mechanism may take place on the surface of  $\text{TiO}_2$ . Table 1.1 summarizes related works on the dye-modified  $\text{TiO}_2$  for the photocatalytic degradation of organic pollutants.

Table 1.1: Related work on dye-modified TiO<sub>2</sub> for the photocatalytic degradation of organic pollutants.

Researcher	Study	Summary	Remarks
(Hilal <i>et al.</i> , 2007)	Modified TiO <sub>2</sub> with TPPHS <sup>a</sup> dye and supported on AC <sup>b</sup> surface for the degradation of phenol and benzoic acid under UV and visible light.	<ul style="list-style-type: none"> <li>All system (naked TiO<sub>2</sub>, TPPHS solution, TiO<sub>2</sub>/TPPHS and AC/TiO<sub>2</sub>/TPPHS) showed low catalytic performance under visible light.</li> <li>The performance of AC/TiO<sub>2</sub>/TPPHS enhanced under UV region.</li> <li>The mechanism was a charge-transfer rather than sensitization.</li> <li>AC adsorb contaminant molecules and bring them closer to the catalytic surface.</li> </ul>	<ul style="list-style-type: none"> <li>TiO<sub>2</sub>, TPPHS and AC were physically mixed – need additional treatment to remove the particles from the treated water.</li> <li>The photocatalytic performance of the recovered photocatalyst was slower upon reusability.</li> </ul>
(Kuo <i>et al.</i> , 2008)	Degrade carbaryl rinsate (insecticide) by solar photocatalysis assisted with MB <sup>c</sup> and RB <sup>d</sup> dyes	<ul style="list-style-type: none"> <li>Direct adsorption of the dye on the TiO<sub>2</sub> surface before undergoes photocatalytic reaction in suspension mode</li> </ul>	<ul style="list-style-type: none"> <li>Need additional treatment to remove the particles from the treated water.</li> <li>Did not discuss about the regeneration and reusability of the photocatalyst.</li> </ul>
(Vinu <i>et al.</i> , 2010)	Prepared a combustion synthesized nano TiO <sub>2</sub> sensitized EY <sup>e</sup> and FL <sup>f</sup> dyes for the degradation of phenolic compounds (phenol, 4-CP <sup>g</sup> , DCP <sup>h</sup> , and TCP <sup>i</sup> ) under visible light.	<ul style="list-style-type: none"> <li>The rate of degradation was higher in the presence of EY as compared to FL.</li> <li>The order of degradation : 4-CP &gt; TCP &gt; DCP &gt; phenol.</li> <li>Different phenolic and dye intermediates were identified by LC-MS.</li> <li>Detailed mechanisms and intermediates were presented.</li> </ul>	<ul style="list-style-type: none"> <li>The dye and TiO<sub>2</sub> were mixed with the pollutants – need additional treatment to remove the particles from the treated water.</li> <li>Complete mineralization was not achieved (TOC is high) due to the photobleaching of the dye-sensitizer.</li> </ul>

Table 1.1 Continued

(Zyoud <i>et al.</i> , 2011)	Developed a TiO <sub>2</sub> /anthocyanin (natural dye) system supported on activated carbon (AC) particles for the degradation of MO <sup>I</sup> under visible and solar light simulator.	<ul style="list-style-type: none"> <li>• TiO<sub>2</sub>/anthocyanin shows photocatalytic performance under visible light.</li> <li>• When supported on AC, the efficiency enhanced (due to adsorption of MO) and easy to recover after the reaction.</li> <li>• The sensitizer degrade during the photoreaction but complete mineralization was achieved.</li> <li>• Sensitizer degradation caused deactivation of the supported catalyst on recovery and re-treatment of the recovered catalyst with fresh dye can overcome the problem.</li> </ul>	<ul style="list-style-type: none"> <li>• TiO<sub>2</sub>, anthocyanin and AC were physically mixed – need additional treatment to remove the particles form the treated water.</li> <li>• The AC/TiO<sub>2</sub>/anthocyanin need re-treatment of the recovered catalyst for it to be reusable – the dye-sensitizer undergoes fast photobleaching.</li> <li>• The performance of the recovered AC/TiO<sub>2</sub>/anthocyanin was slower than the fresh catalyst.</li> </ul>
------------------------------	---	---	--

Table 1.1 Continued

(Qin <i>et al.</i> , 2011)	Sensitized bifunctional TiO <sub>2</sub> film with a N719 dye for the degradation of two reactors containing 4-CP under visible light irradiation with experimental set-up similar to dye-sensitized solar cells (DSSC).	<ul style="list-style-type: none"> <li>• The degradation was improved by the addition of FeSO<sub>4</sub> – Fe<sup>2+</sup> react with H<sub>2</sub>O<sub>2</sub> to increase the production of OH<sup>•</sup>.</li> <li>• High degradation efficiency was obtained when TiO<sub>2</sub> film based on glass was used – electrons induced by light can directly transfer from the dye-sensitized zone to the degradation zone through the TiO<sub>2</sub> film.</li> <li>• The bifunctionalized TiO<sub>2</sub> film was reusable for at least five cycles of usage.</li> </ul>	<ul style="list-style-type: none"> <li>• Difficult experimental set-up.</li> <li>• The use of metal-dye which is hazardous and expensive.</li> </ul>
----------------------------	--	---	--

<sup>a</sup> 2,4,6-triphenylpyrilium hydrogen sulfate

<sup>b</sup> Activated carbon

<sup>c</sup> Methylene blue

<sup>d</sup> Rose bengal

<sup>e</sup> Eosin Y

<sup>f</sup> Fluorescein

<sup>g</sup> 4-chlorophenol

<sup>h</sup> 2,4-dichlorophenol

<sup>i</sup> 2,4,6-trichlorophenol

<sup>j</sup> Methyl orange

## 1.5 Chitosan (CS) biopolymer

Chitosan [ $\beta$ -(1-4)-2-amino-2-deoxy-D-glucose] or CS is a cationic biopolymer manufactured at industrial scales by the deacetylation of chitin. Chitin is the most abundant natural polysaccharide that can be found as the main component on shell of crustaceans such as crab or shrimp shell. To produce chitin, the crustacean shells are subjected to chemical and enzymatic deproteinization, acid treatment for dissolution of calcium carbonate, and discoloration to remove residual pigments. On the other hand, CS is produced by deacetylating chitin in sodium hydroxide as shown in Figure 1.7.

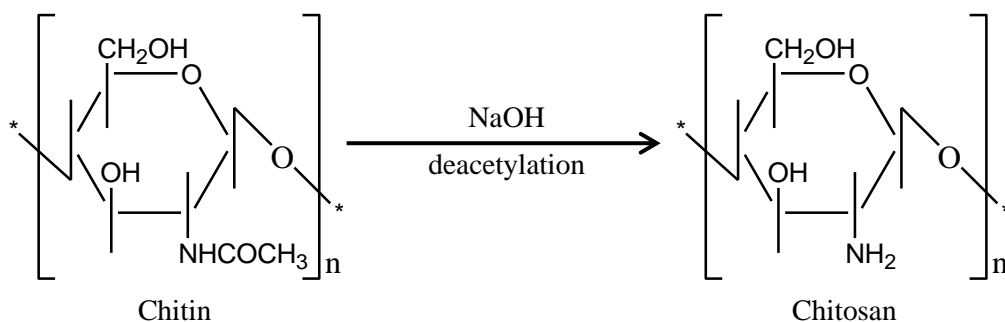


Figure 1.7: Scheme of chemical deacetylation of chitin to produce chitosan.

### 1.5.1 Properties of CS

CS has become the attention of many researchers due to its low-cost, abundance, non-toxicity, hydrophilicity, biocompatibility, biodegradability and anti-bacterial properties (Kumar, 2000; Chiou and Li, 2002). It contains large number of functional or reactive groups, such as amino- and hydroxyl groups, which serve as coordination and reaction sites. Modification of CS such as cross-linking (Beppu *et al.*, 2007; Baroni *et al.*, 2008; Ngah and Fatinathan, 2008; Ngah *et al.*, 2008; Chen

and Chen, 2009), grafting (Chao *et al.*, 2004; Crini *et al.*, 2008) and protonation (Viswanathan *et al.*, 2009), were also possible to improve its adsorption ability, chemical and mechanical properties. In addition, the chemical structure and optical properties of CS can be altered by photo-modification in order to reduce the average molecular weight and viscosity, increase its water-solubility, as well as to improve its optical and spectral sensitivity (Huang *et al.*, 2007; Yue *et al.*, 2009; Duy *et al.*, 2011; Nawi *et al.*, 2011a; Hien *et al.*, 2012; Jawad and Nawi, 2012a; Jawad and Nawi, 2012b). Besides, CS can be easily molded in several shapes from water soluble forms to solid forms (gels, beads, flakes, fibers, membranes, etc.) in order to suit its various types of applications.

### **1.5.2 Applications of CS**

CS has a diverse range of applications in the fields of agriculture, biomedicine and pharmaceutical, biotechnology, cosmetic, food, pulp and paper, textile as well as environmental remediation (Kumar, 2000; Rinaudo, 2006). It is widely applied in water and wastewater treatment as coagulating, flocculating and chelating agents (Crini and Badot, 2008) due to its interesting properties as listed in Table 1.2.

CS has demonstrated to be one of the most promising adsorbents in wastewater treatment for its adsorption of heavy metals (Wu *et al.*, 2000; Ngah *et al.*, 2005; Ngah and Fatinathan, 2008), organic compounds (Ahmad *et al.*, 2005; Chang and Juang, 2005) and dyes (Chatterjee *et al.*, 2007; Crini *et al.*, 2008; Rosa *et al.*, 2008). In fact, CS has also been used as a polymer-based catalyst (Šuláková *et al.*,

2007; Castro *et al.*, 2009), immobilization matrices for the construction of biosensors (Azmi *et al.*, 2009), enzymes (Zhang *et al.*, 2009a; Liu *et al.*, 2012), and photosensitizers (Bonnett *et al.*, 2006).

Table 1.2: Principal properties of CS in relation to its use in water and waste treatment applications (Renault *et al.*, 2009).

Principal characteristics	Potential applications
<ul style="list-style-type: none"> <li>• Non-toxic</li> <li>• Biodegradable</li> <li>• Renewable resource</li> <li>• Ecologically acceptable polymer (eliminating synthetic polymers, environmentally friendly)</li> <li>• Efficient against bacteria, viruses, fungi</li> <li>• Formation of salts with organic and inorganic acids</li> <li>• Ability to form hydrogen bonds intermolecularly</li> <li>• Ability to encapsulate</li> <li>• Removal of pollutants with outstanding pollutants-binding capacities</li> </ul>	<ul style="list-style-type: none"> <li>• Flocculant to clarify water (drinking water, pools)</li> <li>• Reduction of turbidity in food processing effluents</li> <li>• Coagulation of suspended solids, mineral and organic suspensions</li> <li>• Flocculation of bacterial suspensions</li> <li>• Interactions with negatively charged molecules</li> <li>• Recovery of valuable products (proteins, etc.)</li> <li>• Chelation of metal ions</li> <li>• Removal of dye molecules by adsorption processes</li> <li>• Reduction of odors</li> <li>• Sludge treatment</li> <li>• Filtration and separation</li> <li>• Polymer assisted ultrafiltration</li> </ul>

### 1.5.3 Works related to CS with TiO<sub>2</sub> semiconductor

In recent years, several studies have revealed that CS biopolymer exhibited multi-functional performances with TiO<sub>2</sub> in heterogeneous photocatalysis technologies as listed in Table 1.3. CS has also been combined with other photocatalysts such as zinc oxide (Salehi *et al.*, 2010; Zhu *et al.*, 2012), niobium oxide (Torres *et al.*, 2006), cuprous oxide (Chen *et al.*, 2008) and cadmium sulphide



(Jiang *et al.*, 2009; Zhu *et al.*, 2009) in order to enhance the photocatalytic degradation of organic pollutants and heavy metals.

## **1.6 Phenol as a model pollutant**

Organics such as phenol are the most common pollutant emitted into the surface water. It is introduced into water from industries such as pesticides, coal conversion, petroleum, petrochemicals, paint, polymer resin, pharmaceuticals, and also from domestic wastewater. It is a high priority pollutant due to its toxicity even at low concentration, possible accumulation in the environment leading to the formation of substituted compounds during disinfection and oxidation processes (Busca *et al.*, 2008). It can cause unpleasant taste and odor of drinking water and can exert negative effects on different biological processes (Bhatnagar and Sillanpää, 2009). In Malaysia, the Department of Environment (DOE) has set a national guideline for phenolics content which specifies that its concentration in the drinking water should not exceed  $0.001 \text{ mg L}^{-1}$  (D.O.E., 2010).

Several review papers focusing on the recent development of heterogeneous photocatalysis under visible and solar light for the photocatalytic degradation of phenol and its derivatives in wastewater have been published (Ahmed *et al.*, 2010; Ahmed *et al.*, 2011; Grabowska *et al.*, 2012). Degradation of phenol by  $\text{TiO}_2$  photocatalyst system is the most widely investigated (Table 1.4).